Supplemental information for

# Capacity fading mechanism of tin phosphide anodes in sodium-ion batteries

Ronnie Mogensen, Julia Maibach, Andrew J. Naylor, Reza Younesi*

Department of Chemistry-Ångström Laboratory, Uppsala University, Box 538, SE-75121 Uppsala, Sweden
E-mail: reza.younesi@kemi.uu.se

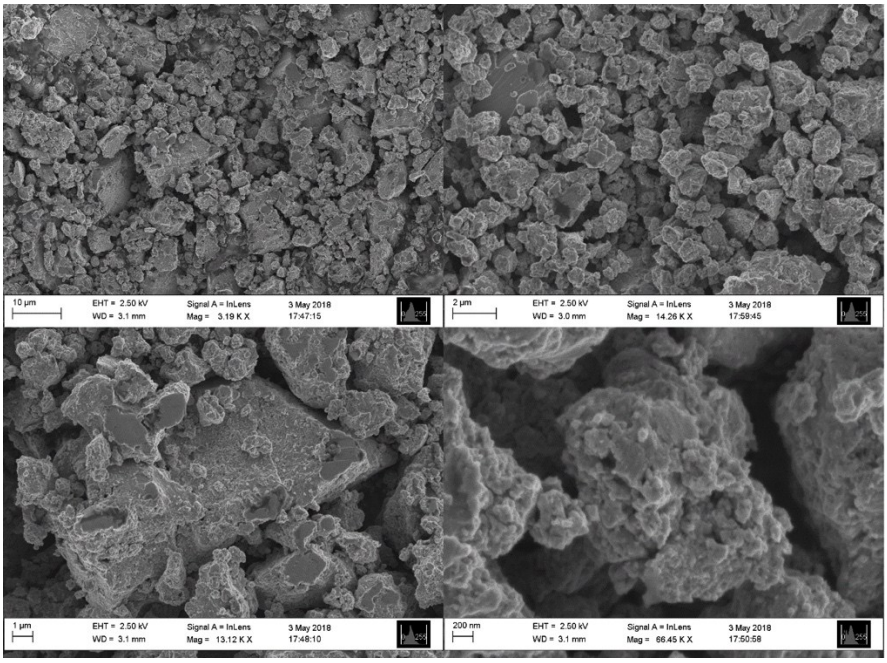


*S1. SEM images of the pristine powder used to manufacture tin phosphide electrodes obtained using a Zeiss 1550 SEM using the in-lens detector and an acceleration voltage of 2.5 kV.*

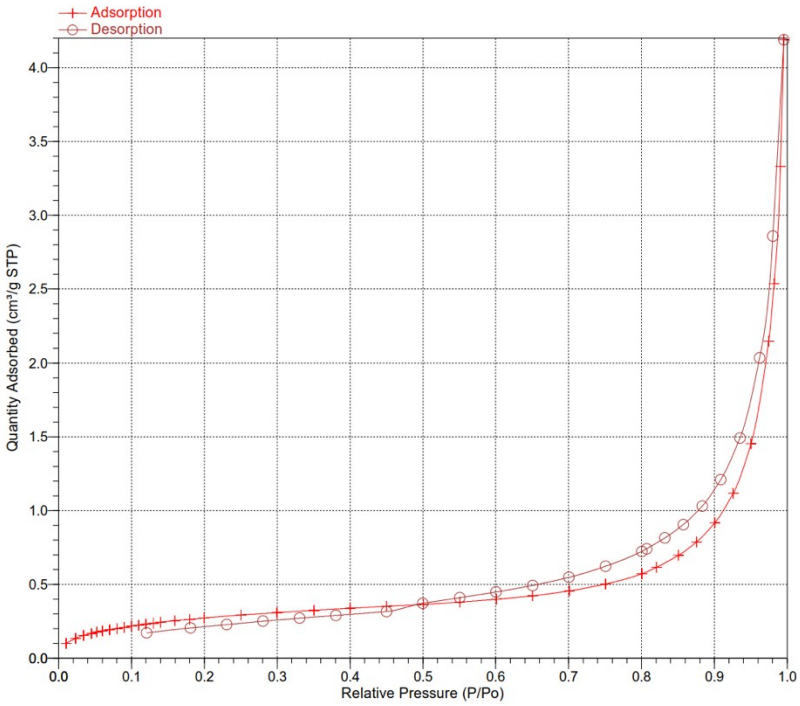


*S2. $N_2$ adsorbtion-desorbtion isotherms of pristine tin phosphide powder measured on a micromeritics ASAP 2020 instrument. The sample mass was 0.995 g and BET Surface area was determined to 0.9623 $m^2.g^{-1}$.*

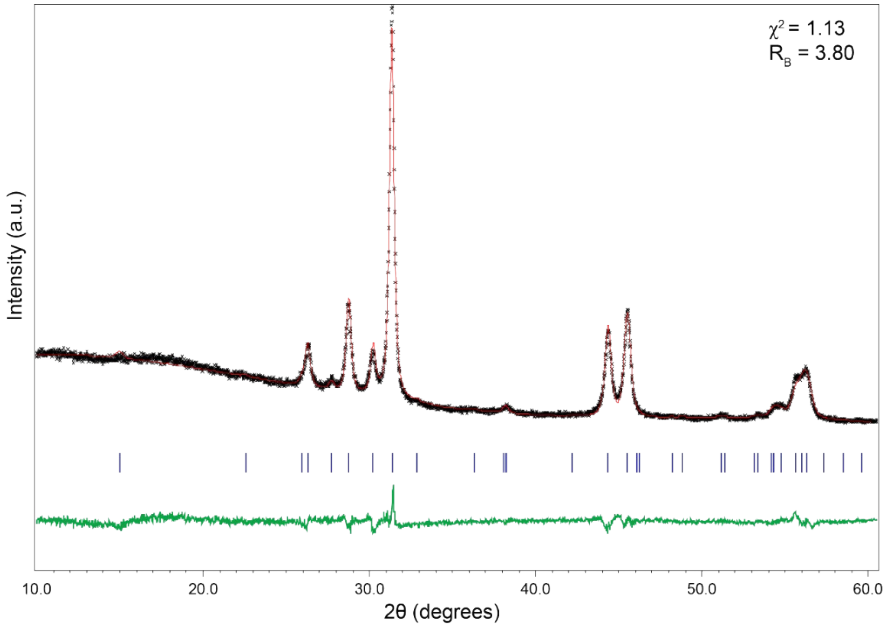


*S3. X-ray diffraction pattern of the pristine $Sn_4P_3$ powder used to manufacture tin phosphide electrode. Rietveld refinement (red line) of pure $Sn_4P_3$ powder collected with single wavelength Cu Kα radiation (λ = 1.5418 Å). The positions of the allowed reflections are marked with vertical blue lines. The green curve indicates the difference between the observed data and refined model. This diffractogram is from our previous work: R. Mogensen, J. Maibach, W. R. Brant, D. Brandell and R. Younesi, Electrochim. Acta, 2017,* ***245****, 696–704.*

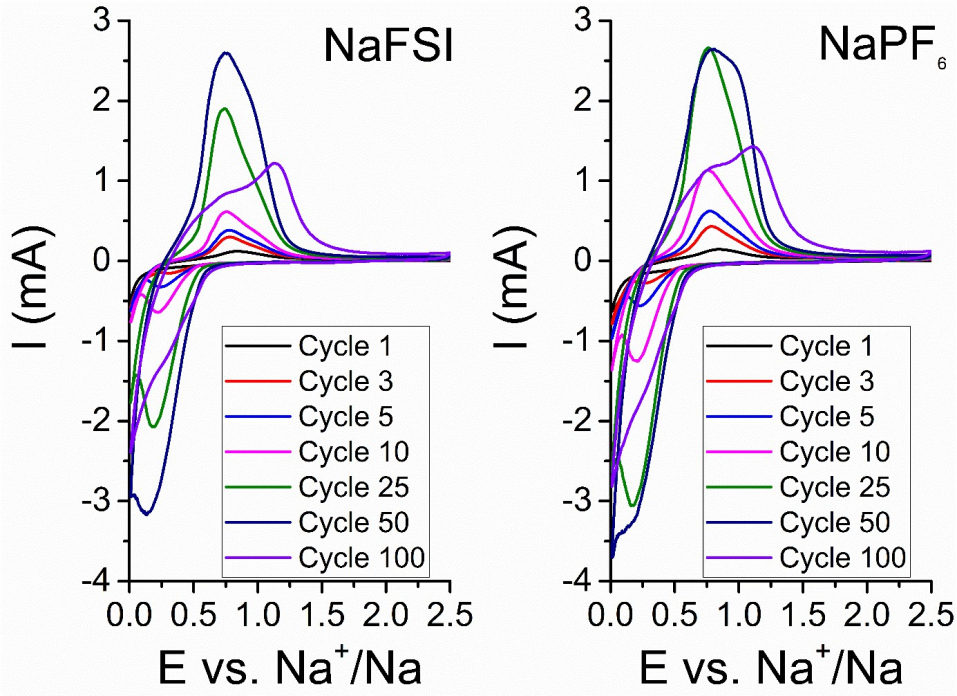


*S4. Cyclic voltammetry on the same samples as in the main text but with selected cycles up to cycle 100 displayed. Electrodes using NaFSI electrolyte (left) and $NaPF_6$ electrolyte (right) were both cycled at1 $mV.S^{-1}$ scan rate between 0.01 V & 2.5 V.*

Figure S5 displays discharge and charge capacities for cells with either $NaPF_6$ or NaFSI electrolyte salts. The relaxation/pause was applied after 10 cycles. While the tests showed clear and repeatable results in all the cells with $NaPF_6$ salt, the technique could not resolve any difference for the NaFSI salt and four different cells are displayed to show that this was consistent behavior for all the cells with NaFSI.

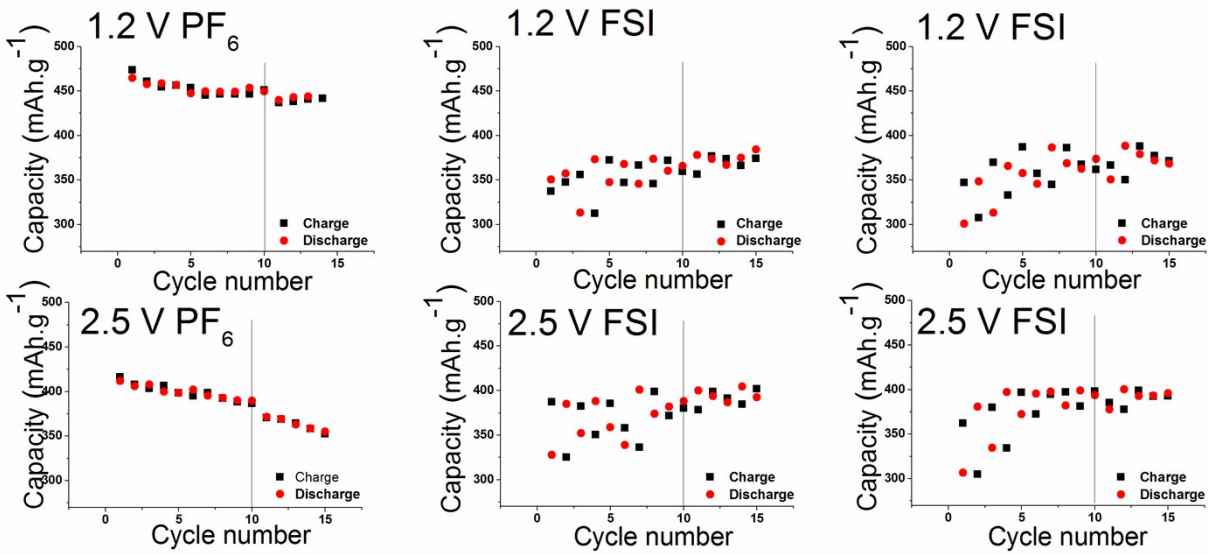


*S5. Cell capacities before and after pause/relaxation for all the tests including the results for cells with NaFSI.*

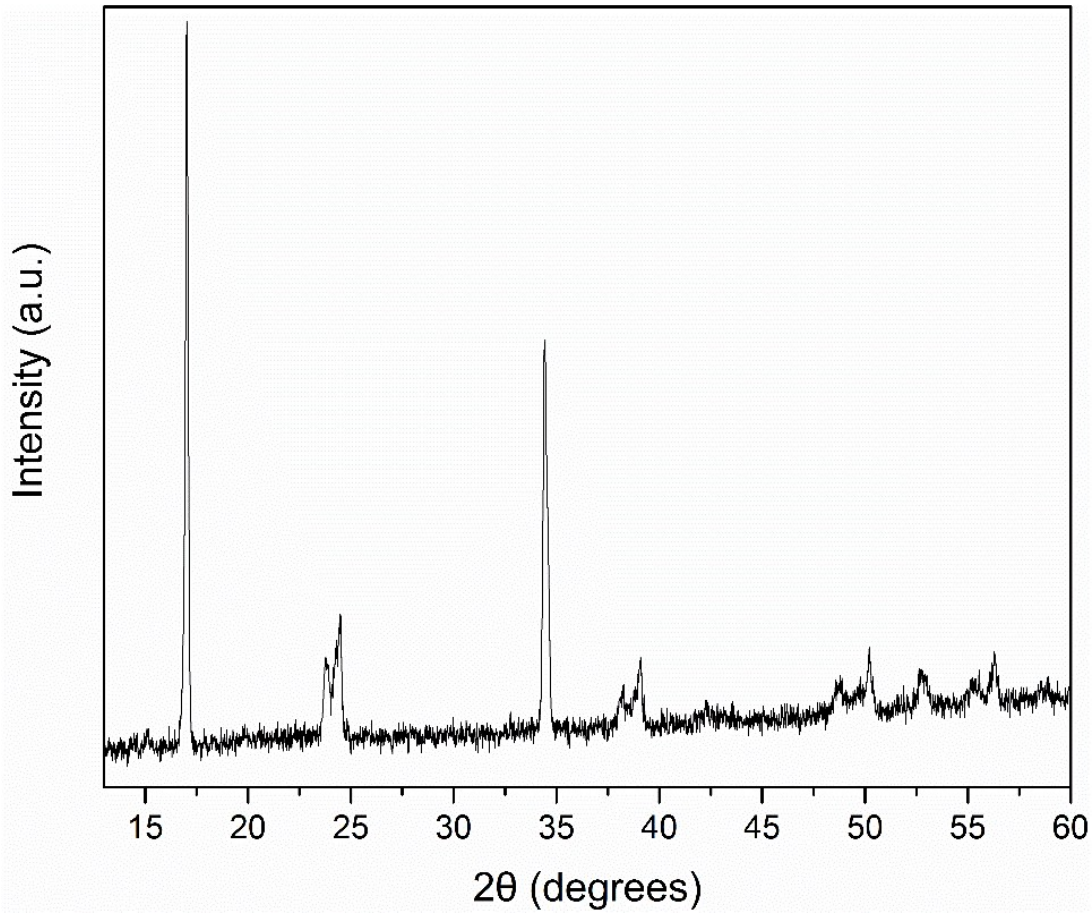


*S6. X-ray powder diffraction pattern of the pristine Prussian blue powder used to manufacture cathodes for full cells. Collected using single wavelength Cu Kα radiation (λ = 1.5418 Å).*

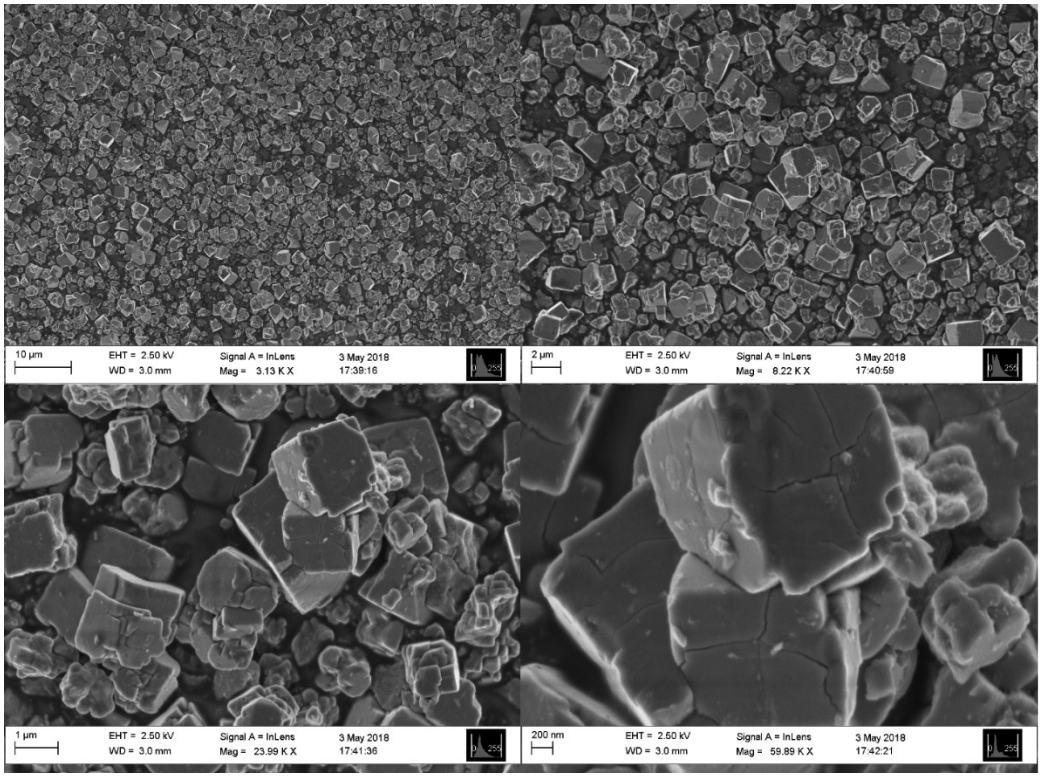


*S7. SEM images of pristine powder used to manufacture Prussian blue cathodes obtained using a Zeiss 1550 SEM using the in-lens detector and an acceleration voltage of 2.5 kV.*

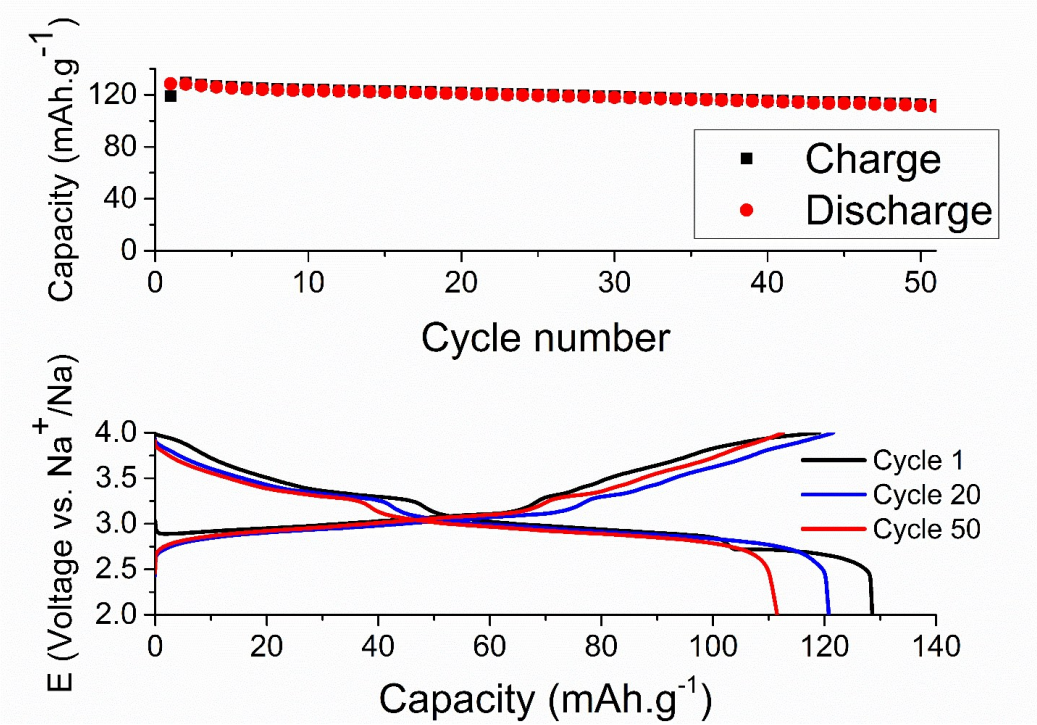


*S8. Galvanostatic cycling data from a half-cell consisting of Prussian blue vs. sodium metal. The cell was cycled at 10 mA.g$^{-1}$ current density using 1 M $NaPF_6$ in EC:DEC electrolyte with 10 wt% FEC additive. Mass loading of the 13 mm electrode was 9.3 mg Prussian blue.*

HAXPES:

The HAXPES spectra using the photon energy of 6015 eV was performed on the same samples as in the main text. Since the photon energy of 6015 eV results in deeper probing depth, some differences appear such as in the case for Sn 3d where hardly any difference between the cut-off potentials can be seen. For all other elements the results are very similar to the 2005 eV spectra.

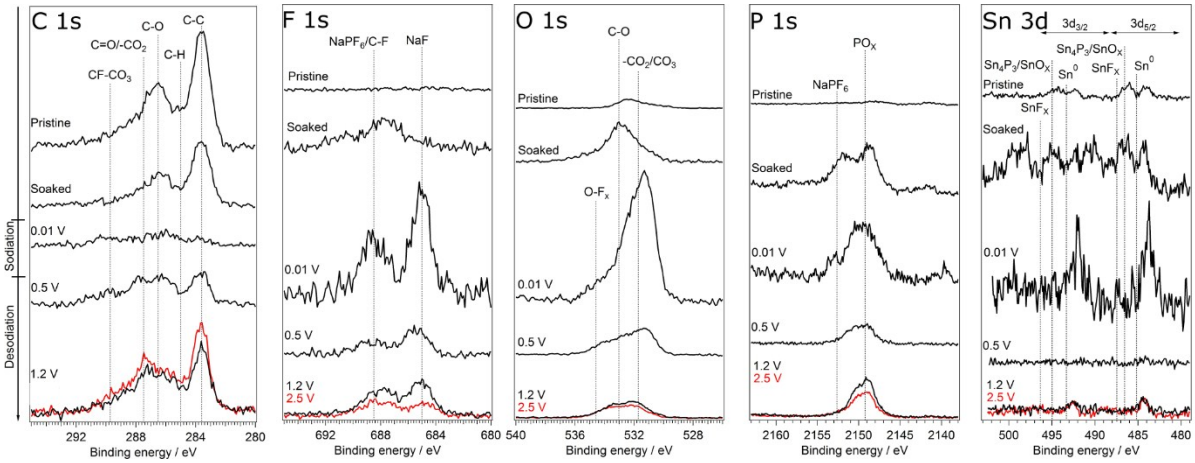


*S9. HAXPES spectra of tin-phosphide electrodes measured with photon energy of 6015 eV.*

As the lower desodiation voltage could lead to an unintentional form of capacity limitation, we tested it by adding together all discharge capacities up to cycle 50 where all cells using the high desodiation potential showed severe capacity drop. To the left in figure S10 the accumulated discharge capacity is plotted. The discharge capacity is from the cells displayed to the right in the capacity *vs.* cycle number plot. The cells using the lower desodiation potential continue to show significant discharge capacities well after 50 cycles while their high desodiation potential counterparts provided very limited capacities per cycle after this point.

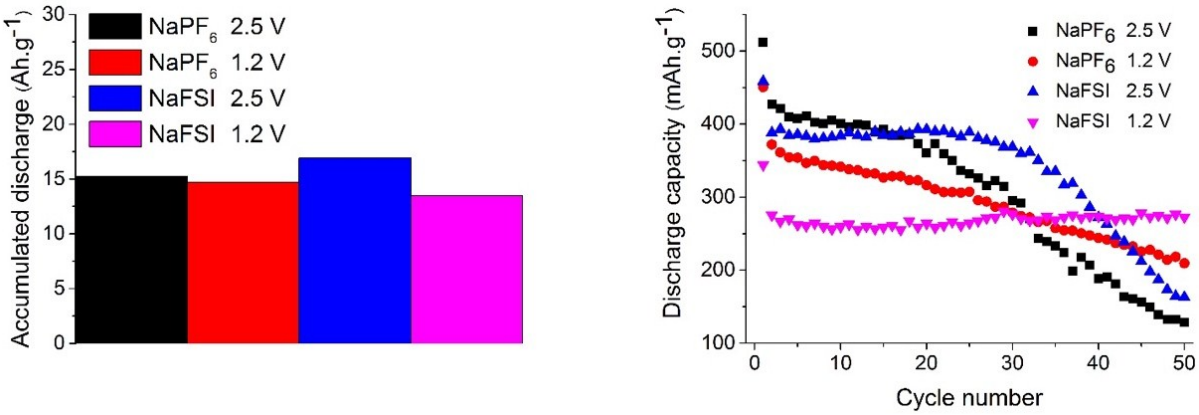


*S10. Accumulated discharge capacity of half-cells cycled galvanostatically for 50 cycles (left) and cycling data for source cells (right).*